Scientia Iranica B (2015) 22(1), 208–219

Sharif University of Technology
Scientia Iranica
Transactions B: Mechanical Engineering
www.scientiairanica.com

Natural circulation in vertical porous annular enclosure with heat generation

M. Taherzadeh[a,*] and M.S. Saidi[b]

a. *Department of Energy Engineering, Sharif University of Technology, Tehran, P.O. Box 11365-11155, Iran.*
b. *Department of Mechanical Engineering, Sharif University of Technology, Tehran, P.O. Box 11365-11155, Iran.*

Received 13 October 2013; received in revised form 23 April 2013; accepted 19 May 2014

KEYWORDS
Natural circulation;
Porous media;
Heat generation;
Annular enclosure;
Finite volume method

Abstract. Natural convection flow is considered in an annular enclosure filled with a fluid-saturated porous medium. The top and bottom horizontal walls are insulated, while the outer vertical wall is cooled with a constant temperature, and a linear temperature gradient is applied to the inner vertical wall. Dimensionless equations are solved numerically using the Finite Volume Method (FVM) on a collocated non-uniform, orthogonal grid. The Darcy-Forchheimer model is used to simulate the momentum transfer in the porous medium. The effect of Rayleigh, Darcy, Prandtl, solid-fluid Nusselt, heat generation parameters and effective conductivity ratio of phases on the streamlines and isotherms are presented, as well as on the rate of heat transfer from the inner and outer vertical walls of the enclosure. It is concluded that at low values of the effective conductivity ratio of phases, only the heat generation parameter has a significant effect on the temperature field of the solid phase and the heat transfer from inner and outer vertical walls. An analytical solution is obtained for this case and compared with the numerical solution. The results show good agreement with each other.

1. Introduction

Porous media and the corresponding heat transfer phenomena have attracted considerable attention, due to their relevance to a wide variety of applications in engineering and science, such as underground heat exchangers for energy saving, oil extraction, solar collectors, nuclear reactors, cooling electronic devices, thermal insulations, geothermal energy, etc. These applications are discussed and reviewed by Nield and Bejan [1], Ingham and Pop [2-4], Vafai [5] and Ingham et al. [6].

As the result of thermal boundary conditions and internal heat generation, natural circulation can be developed in a porous environment. In this context, buoyancy driven phenomena in porous media are actively under investigation. Mealey and Merkin [7] investigated steady convective flow within a porous square region with heat generation, and two constant temperature vertical walls and two adiabatic horizontal walls. They concluded that natural convection can occur in a limited range of Ra number and volumetric heat power. Tahmasebi et al. [8] considered a similar problem and investigated the effects of Ra number and volumetric heat power on the strength of vortices and maximum temperature in a porous cavity. Natural convection in enclosures partially filled with a heat-generating porous medium is numerically solved by Du and Bilge [9], and Kim et al. [10]. Kim and Hyun [11] investigated buoyant convection in a rectangular cavity filled with heat-generating porous medium. They used a power-law non-Newtonian fluid in an enclosure and concluded that, as the enclosure aspect ratio increases or the power-law model increases, the flow

*. *Corresponding author. Tel./Fax: +98 21 66166101*
E-mail addresses: Taherzadeh@energy.sharif.ir (M. Taherzadeh); mssaidi@sharif.ir (M.S. Saidi)

enters the boundary-layer regime at higher Reynolds number. Rao and Wang [12] and Haajizadeh et al. [13] considered a uniform heat generation term across an enclosure with isothermal vertical walls and adiabatic horizontal walls. Stewart et al. [14] modeled the case where the lower half of a rectangular container was adiabatic and the upper half was isothermal. Joshi et al. [15] presented an analytic solution for small Rayleigh number for a finite container with isothermal walls, again, for uniform heat generation within the porous medium. Boundary-layer (large Rayleigh) flows in porous media with, also, internal heat generation, is treated by Magyari et al. [16,17].

Very few investigations have been made in the past to focus on natural convection in porous medium with heat generation. In the present work, the steady free convective flow within a porous annular enclosure with heat generation is investigated, where horizontal walls are insulated, while the outer vertical wall is cooled with constant temperature, θ_0, and the inner vertical wall is set at constant temperature, θ_δ, at the upper end, linearly decreasing to θ_0 at the lower end. The Darcy-Forchheimer model is used to simulate the momentum transfer in the porous medium. This model was developed by Vafai and Tien [18] in order to bridge the gaps between Darcy and Navier-Stokes equations. It is known that Darcy's law is an empirical formula relating to the pressure gradient, the gravitational force and the bulk viscous resistance in porous media. Thus, the mathematical formulations based on Darcy's law neglect the effects of a solid boundary or inertia forces on fluid flow and heat transfer through porous media. In general, the inertia and boundary effects become significant when the fluid velocity is high, the heat transfer is considered in the near wall region [19], and the Darcy-Forchheimer model describes the effect of inertia as well as viscous forces in porous media. In addition, in the present work, the impact of six non-dimensional parameters, including Rayleigh, Darcy, Prandtl, solid-fluid Nusselt, heat generation parameters and the effective conductivity ratio of phases, on the streamlines and isotherms are investigated, as well as on the rate of heat transfer from the inner and outer vertical walls of the enclosure.

The numerical calculations were performed using the THERMOUS code, which is an in-house developing software for thermal-hydraulic modeling of multi-phase flow in porous media.

2. Problem formulation

Consider an annular enclosure filled with a porous material, which generates heat. The geometry of the problem, together with the coordinate system is illustrated in Figure 1. The physical properties are assumed constant, except the density in the buoyancy force term, which is satisfied by the Boussinesq approximation. Regarding the axisymmetric configuration of the problem, governing mass and momentum conservation equations for the fluid phase can be written as:

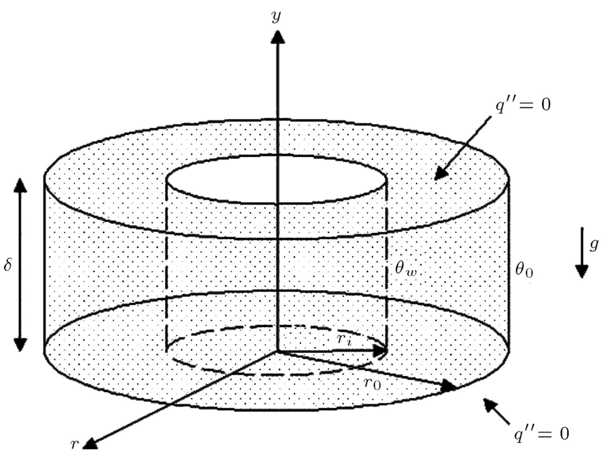

Figure 1. Geometry of the problem and its associated boundary conditions.

$$\frac{1}{r}\frac{\partial ru}{\partial r}+\frac{\partial v}{\partial y}=0, \tag{1}$$

$$\frac{1}{r}\frac{\partial ruu}{\partial r}+\frac{\partial vu}{\partial y}=-\frac{1}{\rho}\frac{\partial p}{\partial r}+\upsilon\left(\frac{1}{r}\frac{\partial}{\partial r}\left(r\frac{\partial u}{\partial r}\right)+\frac{\partial}{\partial y}\left(\frac{\partial u}{\partial y}\right)-\frac{u}{r^2}\right)-\left(\frac{\upsilon}{K}+\frac{c_F}{\sqrt{K}}\sqrt{u^2+v^2}\right)u, \tag{2}$$

$$\frac{1}{r}\frac{\partial ruv}{\partial r}+\frac{\partial vv}{\partial y}=-\frac{1}{\rho}\frac{\partial p}{\partial y}+\upsilon\left(\frac{1}{r}\frac{\partial}{\partial r}\left(r\frac{\partial v}{\partial r}\right)+\frac{\partial}{\partial y}\left(\frac{\partial v}{\partial y}\right)\right)-\left(\frac{\upsilon}{K}+\frac{c_F}{\sqrt{K}}\sqrt{u^2+v^2}\right)v+g\beta(\theta_f-\theta_0). \tag{3}$$

Due to heat generation in the solid phase, its temperature can differ from the liquid phase. Thus, with local thermal non-equilibrium assumption, the energy equation for the liquid phase is:

$$\frac{1}{\alpha_f}\left(\frac{1}{r}\frac{\partial ru\theta_f}{\partial r}+\frac{\partial v\theta_f}{\partial y}\right)=\left(\frac{1}{r}\frac{\partial}{\partial r}\left(r\frac{\partial\theta_f}{\partial r}\right)+\frac{\partial}{\partial y}\left(\frac{\partial\theta_f}{\partial y}\right)\right)+\frac{1}{\varepsilon k_f}h_{sf,eff}(\theta_s-\theta_f), \tag{4}$$

for the solid phase is:

$$\left(\frac{1}{r}\frac{\partial}{\partial r}\left(r\frac{\partial \theta_s}{\partial r}\right)+\frac{\partial}{\partial y}\left(\frac{\partial \theta_s}{\partial y}\right)\right)$$
$$-\frac{1}{(1-\varepsilon)k_s}h_{sf,eff}(\theta_s-\theta_f)+\frac{1}{(1-\varepsilon)k_s}q_s'''=0. \quad (5)$$

Boundary conditions are:

$$u=v=0 \qquad \text{for all boundaries,}$$
$$\theta_f=\theta_s=\theta_0 \qquad \text{for} \quad r=r_o,$$
$$\theta_f=\theta_s=\theta_w=(\theta_\delta-\theta_0)\frac{y}{\delta}+\theta_0 \qquad \text{for} \quad r=r_i,$$
$$\varepsilon k_f\frac{\partial \theta_f}{\partial r}+(1-\varepsilon)k_s\frac{\partial \theta_s}{\partial r}=0; \quad \theta_s=\theta_f$$
$$\text{for} \quad y=y_0 \text{ and } y=\delta. \quad (6)$$

Using the following change of variables:

$$\delta=r_o-r_i, \qquad R=\frac{r}{\delta}, \qquad Y=\frac{y}{\delta},$$
$$U=\frac{u\delta}{\alpha_f}, \qquad V=\frac{v\delta}{\alpha_f}, \qquad T_f=\frac{\theta_f-\theta_0}{\theta_\delta-\theta_0},$$
$$T_s=\frac{\theta_s-\theta_0}{\theta_\delta-\theta_0}, \qquad \gamma_s=\frac{q_s'''\delta^2}{(1-\varepsilon)k_s(\theta_\delta-\theta_0)},$$
$$P=\frac{p\delta^2}{\rho_f\alpha_f^2}, \qquad \mathrm{Pr}=\frac{\upsilon}{\alpha_f}, \qquad \mathrm{Da}=\frac{K}{\delta^2},$$
$$\mathrm{Ra}=\frac{g\beta\delta^3(\theta_\delta-\theta_0)\mathrm{Pr}^2}{\upsilon^2}, \qquad \mathrm{Nu}_{sf}=\frac{h_{sf,eff}\delta^2}{\varepsilon k_f},$$
$$\lambda=\frac{\varepsilon k_f}{(1-\varepsilon)k_s}. \quad (7)$$

The governing (Eqs. (1)-(5)) reduce to non-dimensional form:

$$\frac{1}{R}\frac{\partial RU}{\partial R}+\frac{\partial V}{\partial Y}=0, \quad (8)$$

$$\frac{1}{R}\frac{\partial RUU}{\partial R}+\frac{\partial VU}{\partial Y}=-\frac{\partial P}{\partial R}$$
$$+\mathrm{Pr}\left(\frac{1}{R}\frac{\partial}{\partial R}\left(R\frac{\partial U}{\partial R}\right)+\frac{\partial}{\partial Y}\left(\frac{\partial U}{\partial Y}\right)-\frac{U}{R^2}\right)$$
$$-\left(\frac{\mathrm{Pr}}{\mathrm{Da}}+\frac{c_F}{\sqrt{\mathrm{Da}}}\sqrt{U^2+V^2}\right)U, \quad (9)$$

$$\frac{1}{R}\frac{\partial RUV}{\partial R}+\frac{\partial VV}{\partial Y}=-\frac{\partial P}{\partial Y}$$
$$+\mathrm{Pr}\left(\frac{1}{R}\frac{\partial}{\partial R}\left(R\frac{\partial V}{\partial R}\right)+\frac{\partial}{\partial Y}\left(\frac{\partial V}{\partial Y}\right)\right)$$
$$-\left(\frac{\mathrm{Pr}}{\mathrm{Da}}+\frac{c_F}{\sqrt{\mathrm{Da}}}\sqrt{U^2+V^2}\right)V+\mathrm{Ra}T_f, \quad (10)$$

$$\frac{1}{R}\frac{\partial RUT_f}{\partial R}+\frac{\partial VT_f}{\partial Y}$$
$$=\left(\frac{1}{R}\frac{\partial}{\partial R}\left(R\frac{\partial T_f}{\partial R}\right)+\frac{\partial}{\partial Y}\left(\frac{\partial T_f}{\partial Y}\right)\right)$$
$$+\mathrm{Nu}_{sf}(T_s-T_f), \quad (11)$$

$$\left(\frac{1}{R}\frac{\partial}{\partial R}\left(R\frac{\partial T_s}{\partial R}\right)+\frac{\partial}{\partial Y}\left(\frac{\partial T_s}{\partial Y}\right)\right)$$
$$-\lambda\mathrm{Nu}_{sf}(T_s-T_f)+\gamma_s=0. \quad (12)$$

with the boundary conditions:

$$U=V=0 \qquad \text{for all boundaries,}$$
$$T_f=T_s=0 \qquad \text{for} \quad R=R_o,$$
$$T_f=T_s=T_w=Y \qquad \text{for} \quad R=R_i,$$
$$\frac{\partial T_f}{\partial Y}+\frac{1}{\lambda}\frac{\partial T_s}{\partial Y}=0; \; T_s=T_f \qquad \text{for} \quad Y=0 \text{ and } Y=1. \quad (13)$$

Alazmi and Vafai [20] reviewed a summary of different models for constant wall heat flux. For insulated walls, it is assumed that heat flux is divided between the two phases on the basis of their effective thermal conductivities and their corresponding temperature gradients.

In Eqs. (11) and (12), Nu_{sf} is the local volumetric solid-fluid Nusselt number. Numerous correlations are presented in the literatures for Nu_{sf}. For example, in the case of saturated water, Nu_{sf} could be defined as [21]:

$$\mathrm{Nu}_{sf}=\frac{1}{\varepsilon c_F^2\mathrm{Da}}\Big[\left(7-10\varepsilon+5\varepsilon^2\right)\left(1+0.7\mathrm{Re}^{0.3}\mathrm{Pr}^{0.333}\right)$$
$$+\left(1.33+2.4\varepsilon+1.2\varepsilon^2\right)\mathrm{Re}^{0.7}\mathrm{Pr}^{0.333}\Big], \quad (14)$$

where the Reynolds number is defined as follows:

$$\mathrm{Re}=\frac{c_F\sqrt{\mathrm{Da}}\sqrt{U^2+V^2}}{\mathrm{Pr}}. \quad (15)$$

However, we are interested in investigating the impact of this parameter on flow and heat transfer in an annular enclosure and consider it a general parameter.

3. Numerical solution procedure

The non-dimensional partial differential (Eqs. (8)-(12)), together with the associated boundary conditions, are discretized using the finite volume method on a collocated non-uniform, orthogonal grid. The convective terms of equations are discretized using the QUICK scheme, diffusion and pressure terms and the central difference scheme. The pressure and velocity of Eqs. (8)-(10) are coupled using the SIMPLEC algorithm [22]. The resulting sparse linear systems of equations are solved using the bi-conjugate gradient stabilized method.

When the residuals of mass, momentum and energy equations become less than 1.0E$-$8, the convergence criteria is satisfied. The difference in maximum annulus temperature is found for grid sizes 50×50 and 101×101, to be only 0.5 percentage when $\mathrm{Pr} = 0.5$, $\mathrm{Da} = 1.0\mathrm{E}-6$, $\mathrm{Ra} = 1.0\mathrm{E}+6$, $\varepsilon = 0.4$, $\lambda = 1.0$, $\frac{r_i}{r_o} = 0.1$, $\gamma_s = 20.0$. Therefore, subsequent results are obtained with mesh size 101×101.

Meantime, the developed program has been validated by comparison with various published numerical works. The results for single phase flow with no porous media in a square cavity and axisymmetric cylindrical geometry were compared with [23-25] for different Reynolds and Rayleigh numbers, and agreed very well. Moreover, natural convection in a square cavity filled with a porous medium was investigated and the results compared with [26], which uses the finite element method on a 41×41 grid point. The results agree very well. For example, in the case of $\mathrm{Pr} = 0.71$, $\mathrm{Da} = 1.0\mathrm{E}-4$, $\mathrm{Ra} = 1.0\mathrm{E}+6$ with a grid size 13×13, the average Nu number was obtained at the bottom wall 7.05, whose difference with the reference value is 1.6 percent. Mohammad [27] investigated non-equilibrium natural convection in a differentially heated cavity filled with a saturated porous matrix, and the difference between our results and this reference is very small. For example, in the case of $\mathrm{Pr} = 10$, $\mathrm{Da} = 1.0\mathrm{E}-5$, $\mathrm{Ra} = 1.0\mathrm{E}+8$ and $\frac{k_f}{k_s} = 0.01$, the average Nu number was computed 1.066, which differs only 0.3 percent with the reference value. In addition, validation of the numerical code in annular geometry filled with porous material was performed, and the results for temperature distribution were compared with [28], and the agreement was good. Meantime, the difference between average Nusselt numbers did not exceed 1.5 percent.

In the present work, the effects of Rayleigh number ($\mathrm{Ra} = 1.0\mathrm{E}+3 - 1.0\mathrm{E}+9$), Darcy number ($\mathrm{Da} = 1.0\mathrm{E}-3 - 1.0\mathrm{E}-8$), Prandtl number ($\mathrm{Pr} = 0.71 - 5.0$), local volumetric solid-fluid Nusselt number ($\mathrm{Nu}_{sf} = 1.0\mathrm{E}{-}3{-}1.0\mathrm{E}{+}5$), effective conductivity ratio of phases ($\lambda = 1.0\mathrm{E}-2-1.0\mathrm{E}+1$) and heat generation parameter ($\gamma_s = 0.0 - 20.0$) are investigated, while other dimensionless parameters, including $\varepsilon = 0.4$, and $\frac{r_i}{r_o} = 0.1$, are kept constant.

4. Evaluation of stream function and Nusselt numbers

4.1. Stream function

In the present work, stream function is used to display fluid motion. The relationships between stream function, ψ, and velocity components are as follows [29];

$$U = \frac{1}{R}\frac{\partial\psi}{\partial Y}, \qquad V = -\frac{1}{R}\frac{\partial\psi}{\partial R}. \tag{16}$$

From this definition, it is possible to obtain a single equation for the stream function;

$$\frac{\partial^2\psi}{\partial Y^2} + \frac{\partial^2\psi}{\partial R^2} = \frac{\partial RU}{\partial Y} - \frac{\partial RV}{\partial R}. \tag{17}$$

In Eq. (17), the positive sign of ψ denotes anticlockwise circulation and the negative sign of ψ denotes clockwise circulation. Due to the no slip boundary condition, the value of ψ is set zero for all boundaries.

4.2. Nusselt numbers

The heat transfer from the inner and outer walls of an annular enclosure in terms of local Nusselt numbers for fluid and solid phases, can be obtained as follows;

$$\mathrm{Nu}_{wf} = -\frac{\partial T_f}{\partial R}, \qquad \mathrm{Nu}_{ws} = -\frac{\partial T_s}{\partial R};$$

$$\mathrm{Nu}_{wf} = \frac{h_{wf}\delta}{\varepsilon k_f}, \qquad \mathrm{Nu}_{ws} = \frac{h_{ws}\delta}{(1-\varepsilon)k_s}. \tag{18}$$

Moreover, total heat transfer from the inner and outer walls in terms of local Nusselt number can be obtained as follows:

$$\mathrm{Nu}_w = \mathrm{Nu}_{wf} + \frac{1}{\lambda}\mathrm{Nu}_{ws}. \tag{19}$$

The average Nusselt numbers at inner and outer walls are defined by:

$$\overline{\mathrm{Nu}_w} = \int_0^1 \mathrm{Nu}_w dY. \tag{20}$$

5. Numerical experiments

5.1. Effect of solid-fluid Nusselt number (Nu_{sf})

Figures 2 and 3 show the effect of local volumetric solid-fluid Nusselt number on fluid flow and temperature fields for $\mathrm{Nu}_{sf} = 1.0\mathrm{E}-3$ and $1.0\mathrm{E}+5$, respectively, while $\mathrm{Da} = 1.0\mathrm{E}-3$, $\mathrm{Ra} = 1.0\mathrm{E}+6$, $\gamma_s = 5.0$, $\lambda = 0.01$ and $\mathrm{Pr} = 5.0$.

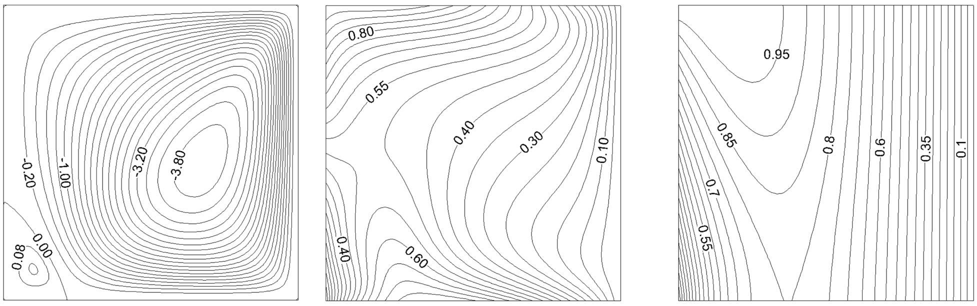

Figure 2. (a) Streamlines, (b) fluid phase isotherms, and (c) solid phase isotherms for $\mathrm{Da} = 1.0\mathrm{E}-3$, $\mathrm{Ra} = 1.0\mathrm{E}+6$, $\gamma_s = 5.0$, $\lambda = 0.01$, $\mathrm{Pr} = 5.0$, and $\mathrm{Nu}_{sf} = 1.0\mathrm{E}-3$.

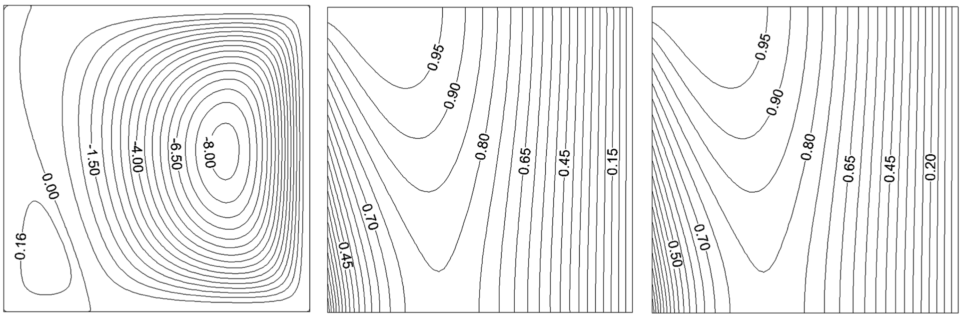

Figure 3. (a) Streamlines, (b) fluid phase isotherms and (c) solid phase isotherms for $\mathrm{Da} = 1.0\mathrm{E}-3$, $\mathrm{Ra} = 1.0\mathrm{E}+6$, $\gamma_s = 5.0$, $\lambda = 0.01$, $\mathrm{Pr} = 5.0$, and $\mathrm{Nu}_{sf} = 1.0\mathrm{E}+5$.

Figures 2(a) and 3(a) illustrate the streamlines of fluid flow. Increasing the local volumetric solid-fluid Nusselt number creates a secondary cell in the left bottom corner of the porous annular enclosure and develops until it fills the left side completely and increases the strength of vortices. Indeed, increasing the Nu_{sf} number increases the heat transfer to the fluid phase, which results in an increase of fluid temperature difference in the annular enclosure and the buoyancy effect.

Figures 2(b) and 3(b) show temperature distribution in the fluid phase. As expected, an increase in Nu_{sf} decreases the convective resistance between two phases and, thus, the temperature difference between the two phases is decreased.

Figures 2(c) and 3(c) illustrate temperature distribution in the solid phase, and it can be seen that Nu_{sf} variation has no significant influence on solid phase temperature. This is due to the low ratio of effective conductivities of phases ($\lambda = 0.01$). Indeed, because of the low conductive resistance of the solid phase compared with fluid phase, most of the generated heat current passes through the solid phase, and the fluid temperature cannot affect solid temperature.

Figure 4 shows the variations of the Nu_{ws} and Nu_{wf} along the inner and outer walls for different values of Nu_{sf}. Variation of Nu_{sf} has no significant effect on the value of Nu_{ws} and this is because of the low conductive resistance of the solid phase compared with the fluid phase. However, the variation of Nu_{sf} has a significant effect on the value of Nu_{wf}, and, for high value of Nu_{sf} ($\mathrm{Nu}_{sf} = 1.0\mathrm{E}+5$), the value of Nu_{wf} and Nu_{ws} will be equal. Also, the value of average wall Nusselt number ($\overline{\mathrm{Nu}_w}$) indicates that with an increase in Nu_{sf}, heat transfer from the inner and outer walls is slightly increased.

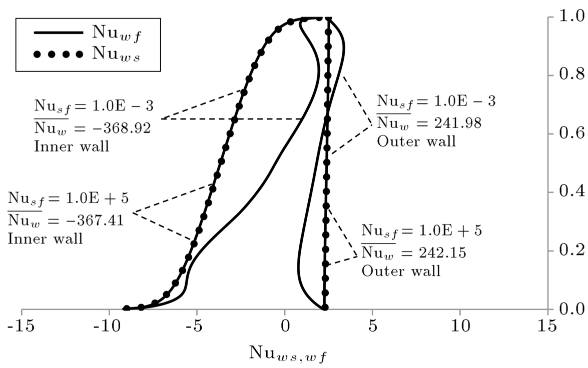

Figure 4. Effect of solid-fluid Nusselt number on heat transfer from inner and outer wall of annular enclosure while $\mathrm{Da} = 1.0\mathrm{E}-3$, $\mathrm{Ra} = 1.0\mathrm{E}+6$, $\gamma_s = 5.0$, $\lambda = 0.01$ and $\mathrm{Pr} = 5.0$.

5.2. Effect of heat generation (γ_s)

Figures 2, 5 and 6 show the effect of the heat generation parameter on fluid flow and temperature fields for

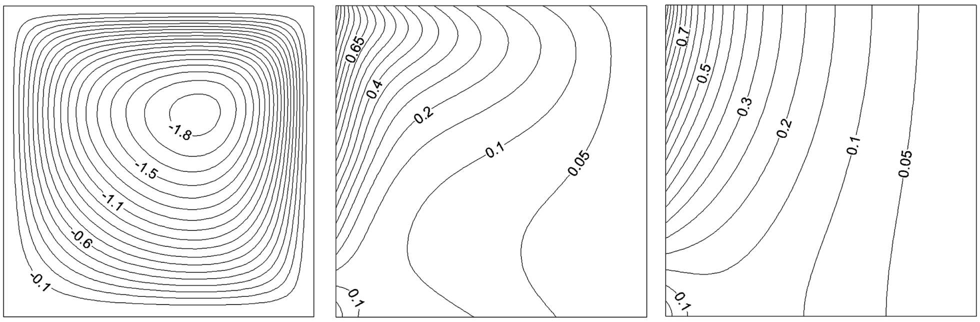

(a) (b) (c)

Figure 5. (a) Streamlines, (b) fluid phase isotherms, and (c) solid phase isotherms for Da = 1.0E − 3, Ra = 1.0E + 6, $\gamma_s = 0.0$, $\lambda = 0.01$, Pr = 5.0 and $\mathrm{Nu}_{sf} = 1.0\mathrm{E}-3$.

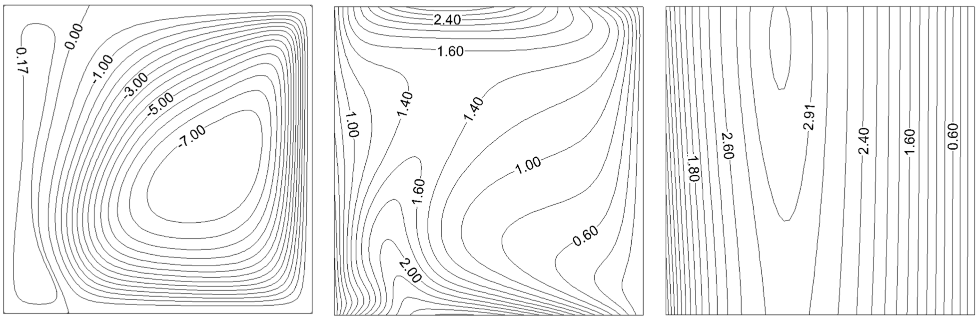

(a) (b) (c)

Figure 6. (a) Streamlines, (b) fluid phase isotherms, and (c) solid phase isotherms for Da = 1.0E − 3, Ra = 1.0E + 6, $\gamma_s = 20.0$, $\lambda = 0.01$, Pr = 5.0 and $\mathrm{Nu}_{sf} = 1.0\mathrm{E}-3$.

$\gamma_s = 5.0$, 0.0 and 20.0, respectively, while Da = 1.0E − 3, Ra = 1.0E + 6, $\lambda = 0.01$, Pr = 5.0 and $\mathrm{Nu}_{sf} = 1.0\mathrm{E}-3$. Figure 5 shows that in the absence of a heat generation parameter, i.e. $\gamma_s = 0.0$, flow and temperature fields are affected by boundary conditions. However, by increasing the heat generation parameter (Figures 2(a) and 6(a)), the strength of vortices increases and a secondary cell is created in the left bottom corner of the porous annular enclosure and develops until fills the left side completely. In Figures 2(b), 2(c), 5(b), 5(c) and 6(b), 6(c), the fluid and solid isotherms show that by increasing the heat generation, the temperature of both phases and the temperature difference between two phases increases. Comparing Figures 2, 5 and 6 indicates that by increasing γ_s, the effect of thermal boundary conditions on flow and temperature fields decreases. Figure 7 shows variation of Nu_{ws} and Nu_{wf} along the inner and outer walls. The value of γ_s has a significant effect on Nu_{ws} and Nu_{wf}. Also, the value of average wall Nusselt number ($\overline{\mathrm{Nu}_w}$) indicates that, with an increase in γ_s, heat transfer from the inner and outer walls is increased.

5.3. Effect of effective conductivity ratio (λ)

Figures 2 and 8 show the effect of heat generation parameter on fluid flow and temperature fields for

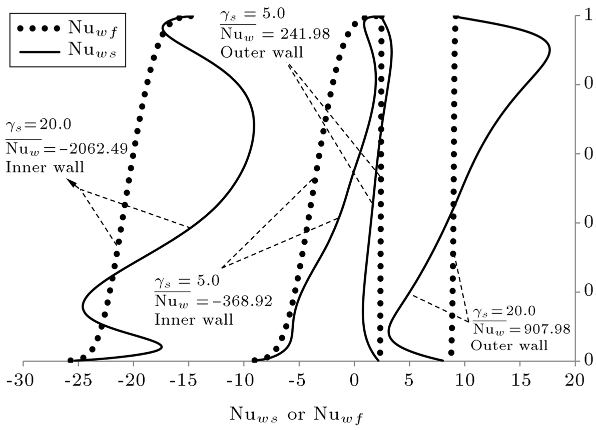

Figure 7. Effect of heat generation on heat transfer from inner and outer wall of annular enclosure while Da = 1.0E − 3, Ra = 1.0E + 6, $\lambda = 0.01$, Pr = 5.0 and $\mathrm{Nu}_{sf} = 1.0\mathrm{E}-3$.

$\lambda = 0.01$ and 10.0, respectively, and for Da = 1.0E − 3, Ra = 1.0E + 6, $\gamma_s = 5.0$, Pr = 5.0 and $\mathrm{Nu}_{sf} = 1.0\mathrm{E}-3$.

Comparing Figures 2(a) and 8(a) show that by increasing the effective conductivity ratio, the secondary cells in the left bottom corner of the porous annular enclosure vanish and the strength of the vortices decreases. Figures 2(b) and 8(b) explain the reason for these phenomena. Due to high effective conductivity or, in another words, the low conductivity resistance

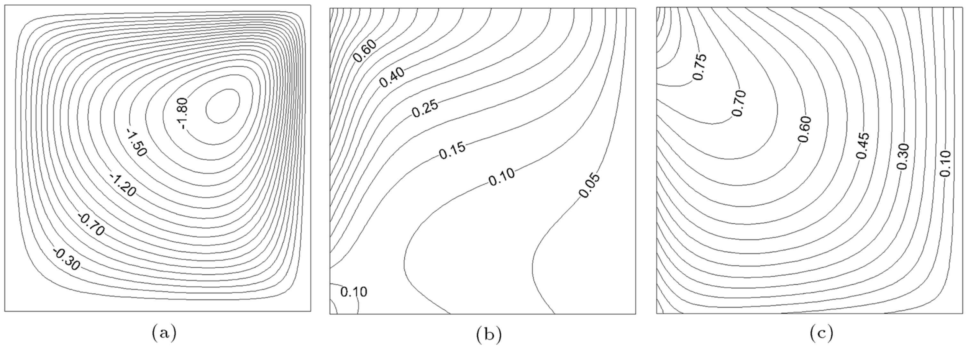

Figure 8. (a) Streamlines, (b) fluid phase isotherms, and (c) solid phase isotherms for Da = 1.0E − 3, Ra = 1.0E + 6, $\gamma_s = 5.0$, $\lambda = 10.0$, Pr = 5.0 and Nu_{sf} = 1.0E − 3.

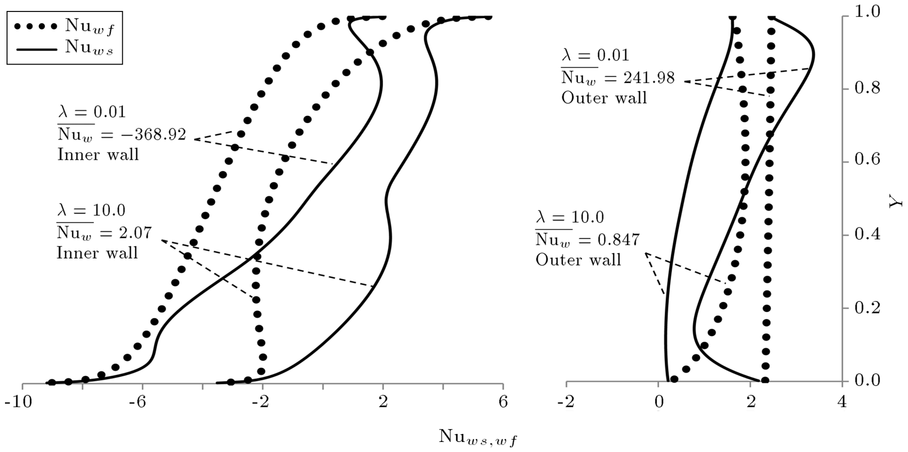

Figure 9. Effect of effective conductivity ratio on heat transfer from inner and outer wall of annular enclosure while Da = 1.0E − 3, Ra = 1.0E + 6, $\gamma_s = 5.0$, Pr = 5.0 and Nu_{sf} = 1.0E − 3.

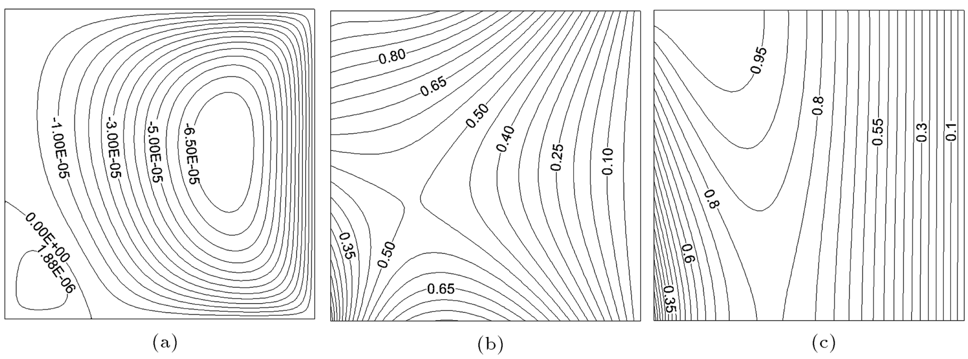

Figure 10. (a) Streamlines, (b) fluid phase isotherms, and (c) solid phase isotherms for Da = 1.0E − 8, Ra = 1.0E + 6, $\gamma_s = 5.0$, $\lambda = 0.01$, Pr = 5.0 and Nu_{sf} = 1.0E − 3.

of the fluid phase compared with the solid phase, the effect of the thermal boundary condition on the fluid phase increases and the temperature gradient and, thus, the buoyancy force in the fluid phase decreases, which causes the strength of the vortices to decrease.

Figures 2(c) and 8(c) show the solid temperature distribution. It is noticed that by increasing λ, due to a reduction in fluid temperature, the solid temperature in the center of the annular enclosure decreases. Figure 9 indicates that increasing λ changes the direction of the heat transfer from the inner wall and decreases the average Nusselt number of the outer wall. Note that although the value of $\overline{\mathrm{Nu}_w}$ on the outer wall decreases, increasing λ increases heat transfer from the outer wall.

5.4. Effect of Darcy number (Da)

Figures 2 and 10 show the effect of Darcy number for Da = 1.0E − 3 and 1.0E − 8, respectively, while Ra = 1.0E + 6, $\gamma_s = 5.0$, $\lambda = 0.01$, Pr = 5.0 and Nu_{sf} = 1.0E − 3. Figures 2(a) and 10(a) indicate that by decreasing the Darcy number, the strength of the vortices decreases. This phenomenon is expected, because decreasing the Darcy number decreases the permeability of the porous media, or, in other words, increases resistance against fluid flow.

Figures 2(b) and 10(b) show temperature distribution in the fluid phase. By decreasing Darcy number and, thus, weak flow circulation, the heat transfer mechanism is changed to conduction. Figures 2(c) and 10(c) indicate that due to the low ratio of effective conductivities of phases, the value of the Darcy number has no significant effect on temperature distribution in the solid phase.

Figure 11 shows variations of the Nu_{ws} and Nu_{wf} along the inner and outer wall and for different values of Da number. Variation of the Da number has no significant effect on the value of Nu_{ws}, and this is because of the low conductive resistance of the solid phase compared to the fluid phase. In addition, Figure 11 indicates that a change of Da number slightly affects heat transfer from inner and outer walls.

5.5. Effect of Rayleigh number (Ra)

Figures 2 and 12 show the effect of Rayleigh number for Ra = 1.0E + 6 and 1.0E + 3, respectively, while Da = 1.0E−3, $\gamma_s = 5.0$, $\lambda = 0.01$, Pr = 5.0 and Nu_{sf} = 1.0E−3. Figure 13 shows variations of Nu_{ws} and Nu_{wf} along the inner and outer walls, and for different values of Ra number. Comparing these figures with Figures 10 and 11 indicates that the effect of Ra number on the flow and temperature field of the annular enclosure is similar to the Da number.

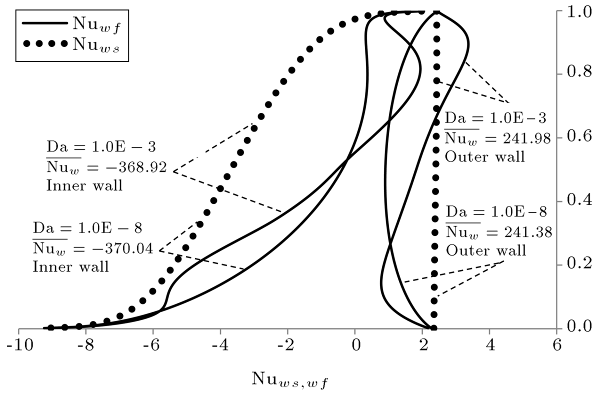

Figure 11. Effect of Darcy number on heat transfer from inner and outer wall of annular enclosure while Ra = 1.0E + 6, $\gamma_s = 5.0$, $\lambda = 0.01$, Pr = 5.0 and Nu_{sf} = 1.0E − 3.

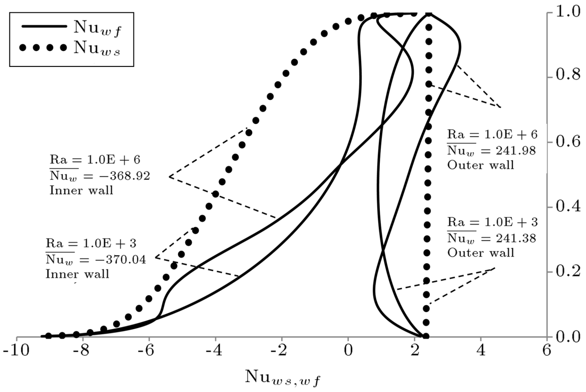

Figure 13. Effect of Rayleigh number on heat transfer from inner and outer wall of annular enclosure while Da = 1.0E − 3, $\gamma_s = 5.0$, $\lambda = 0.01$, Pr = 5.0 and Nu_{sf} = 1.0E − 3.

5.6. Effect of Prandtl number (Pr)

Figures 2 and 14 show the effect of Prandtl number for Pr = 5.0 and 0.71, respectively, while Ra = 1.0E + 6, Da = 1.0E−3, $\gamma_s = 5.0$, $\lambda = 0.01$ and Nu_{sf} = 1.0E−3. Figures 2(a) and 14(a) indicate that by decreasing the Prandtl number, the strength of the vortices increases. Indeed, reduction of the Pr number leads to a reduction in diffusion and enhancement of convection in the momentum transport equations (Eqs. (9) and (10)).

Figures 2(b) and 14(b) show temperature distribution in the fluid phase, and it can be seen that due to enhancement of flow circulation, the fluid temperature in the center of the annular enclosure decreases. Figures 2(c) and 14(c) show temperature distribution in the solid phase, where, due to the low value of λ, there is no significant difference between them.

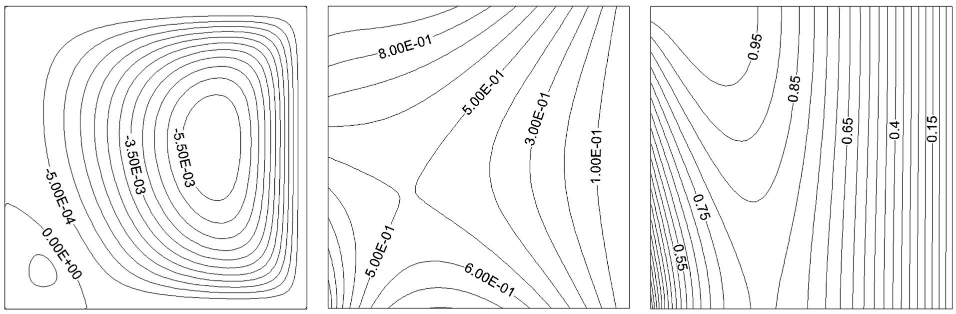

(a) (b) (c)

Figure 12. (a) Streamlines, (b) fluid phase isotherms and (c) solid phase isotherms for Da = 1.0E − 3, Ra = 1.0E + 3, $\gamma_s = 5.0$, $\lambda = 0.01$, Pr = 5.0 and Nu_{sf} = 1.0E − 3.

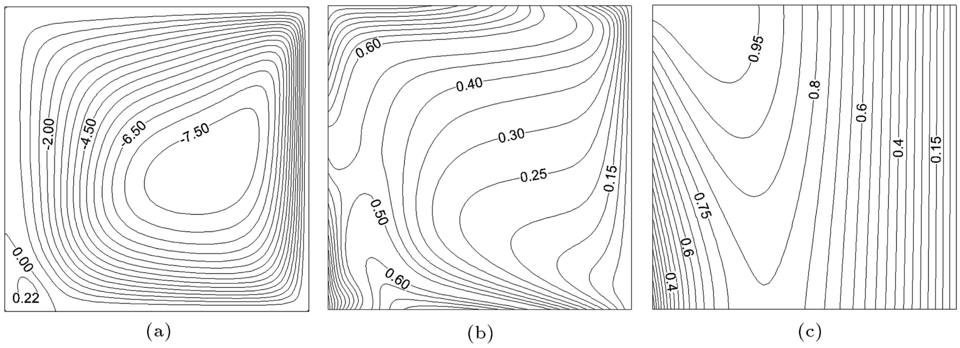

Figure 14. (a) Streamlines, (b) fluid phase isotherms and (c) solid phase isotherms for $\mathrm{Da} = 1.0E-3$, $\mathrm{Ra} = 1.0E+6$, $\gamma_s = 5.0$, $\lambda = 0.01$, $\mathrm{Pr} = 0.71$, $\mathrm{Nu}_{sf} = 1.0E-3$.

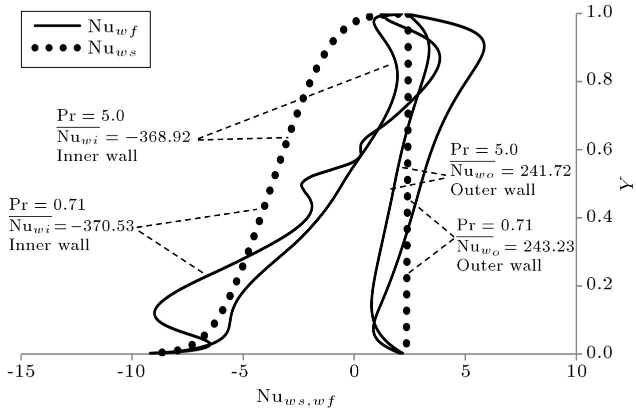

Figure 15. Effect of Prandtl number on heat transfer from inner and outer walls of annular enclosure while $\mathrm{Da} = 1.0\mathrm{E}-3$, $\mathrm{Ra} = 1.0\mathrm{E}+6$, $\gamma_s = 5.0$, $\lambda = 0.01$, $\mathrm{Nu}_{sf} = 1.0\mathrm{E}-3$.

Table 1. Relative change of $\overline{\mathrm{Nu}_w}$ for variation of different non-dimensional parameters.

	$\mathbf{Nu}_{sf}$	**Ra**	**Da**	$\boldsymbol{\gamma_s}$	$\boldsymbol{\lambda}$	**Pr**
Inner wall	0.4%	0.3%	0.3%	99.4%	99.4%	0.4%
Outer wall	0.07%	0.2%	0.2%	275.2%	99.6%	0.6%

Figure 15 shows the effect of Prandtl number on heat transfer from the inner and outer walls of the annular enclosure. It can be seen that decreasing the Pr number increases heat transfer from both inner and outer walls, and, thus, fluid temperature in the annular enclosure is decreased.

6. Analytical solution

In the previous section, the impact of six non-dimensional parameters on the flow and temperature fields, and heat transfer from the inner and outer vertical walls of the annular enclosure were investigated. Table 1 indicates the relative change of $\overline{\mathrm{Nu}_w}$, in percent, for variations of different non-dimensional parameters. From numerical tests, it is concluded that for a low value of an effective conductivity ratio, the impact of the other four non-dimensional parameters, including Ra, Da, Pr and Nu_{sf}, on the solid temperature field and heat transfer from the inner and outer walls is negligible.

As a result, from the above discussion, for low values of λ, it is possible to simplify Eqs. (8)-(12) to Eq. (21), and from an analytical solution, find the solid temperature field and heat transfer from the inner and outer walls of the annular enclosure;

$$\left(\frac{1}{R}\frac{\partial}{\partial R}\left(R\frac{\partial T_s}{\partial R}\right)+\frac{\partial}{\partial Y}\left(\frac{\partial T_s}{\partial Y}\right)\right)+\gamma_s=0. \tag{21}$$

With the boundary conditions:

$$T_s = 0 \qquad \text{for} \quad R = R_o,$$

$$T_s = Y \qquad \text{for} \quad R = R_i,$$

$$\frac{\partial T_s}{\partial Y} = 0 \qquad \text{for} \quad Y = 0 \text{ and } Y = 1. \tag{22}$$

Using Fourier cosine transforms and after applying boundary conditions, the solution of Eq. (21) is:

$$T_s(R,Y) = -\frac{\gamma_s R^2}{4} + A_0 \ln R + B_0$$

$$+\sum_{n=1}^{\infty}\left[A_n I_0(n\pi R) + B_n K_0(n\pi R)\right]\cos(n\pi Y),$$

$$A_0 = \frac{1}{\ln(R_0/R_i)^2}\left[\frac{\gamma_s}{2}(R_o^2 - R_i^2) - 1\right],$$

$$B_0 = \frac{\gamma_s R^2}{4} - \frac{\ln R_0}{\ln\,(R_0/R_i)^2}\left[\frac{\gamma_s}{2}(R_o^2 - R_i^2) - 1\right],$$

$$A_n = \frac{\frac{\delta^*}{K_0(n\pi R_i)}}{\frac{I_0(n\pi R_i)}{K_0(n\pi R_i)} - \frac{I_0(n\pi R_o)}{K_0(n\pi R_o)}},$$

$$B_n = -\frac{I_0(n\pi R_o)}{K_0(n\pi R_o)}A_n,$$

Table 2. Comparison of $\overline{\mathrm{Nu}_w}$ for $\lambda = 0.01$.

γ_s	Numerical		Analytical	
	Inner wall	Outer wall	Inner wall	Outer wall
0.0	195.97	20.57	195.43	19.54
5.0	-368.92	241.98	-373.94	237.61
20.0	-2062.49	907.98	-2082.07	891.79

$$\delta^* = \frac{2}{(n\pi)^2}\left[(-1)^n - 1\right]. \tag{23}$$

Table 2 compares the values of $\overline{\mathrm{Nu}_w}$ found from Eq. (23) for $\gamma_s = 0.0$, 5.0 and 20.0, with numerical results for the same values of γ_s and with Da $= 1.0\mathrm{E}{-3}$, Ra $= 1.0\mathrm{E}+6$, $\lambda = 0.01$, Pr $= 5.0$ and $\mathrm{Nu}_{sf} = 1.0\mathrm{E}-3$. There is good agreement between numerical and analytical results.

7. Conclusions

Numerically, natural convection in a porous annular enclosure with heat generation was investigated. While its horizontal walls are insulated, the outer vertical wall is cooled with a constant temperature, θ_0, and the inner vertical wall has a constant temperature, θ_ε, on the top, which linearly decreases to θ_0 on the bottom. The focus of this study was on the effect of Rayleigh, Darcy, Prandtl, solid-fluid Nusselt and heat generation parameters for low values of effective conductivity ratios. The results show that although variations of Rayleigh, Darcy, Prandtl and solid-fluid Nusselt numbers affects the flow and temperature fields of the fluid phase, at low values of λ, they cannot affect the temperature field of the solid phase. Indeed, at low values of λ, because of the low conductive resistance of the solid phase compared with the fluid phase, most of the generated heat current passes through the solid phase and only the heat generation parameter has a significant effect on the temperature field of the solid phase and the heat transfer from the inner and outer walls. Therefore, it is possible to decouple the solid temperature equation from other equations to find its temperature distribution and heat transfer from the vertical walls. This is important because in most porous media applications, the ratio of heat conductivity coefficients of phases is low, and solving solid energy equations instead of all continuity, momentums and energy equations can be good approximation for heat transfer. An analytical solution for the solid phase temperature equation is presented and the values of average inner and outer wall Nusselt numbers from analytical and numerical solutions are compared. The results show good agreement.

Nomenclature

$c_F = 1.75/\sqrt{150\varepsilon^3}$	Forchheimer dimensionless coefficient
Da	Dimensionless permeability (Darcy number)
g	Acceleration due to gravity
h	Convection heat transfer coefficient
K	Permeability of porous media
k	Thermal conductivity
Nu	Dimensionless convection heat transfer coefficient (Nusselt number)
p	Pressure of fluid
P	Dimensionless pressure of fluid
Pr	Prandtl number
q'''	Volumetric heat generation
r	Radial component of coordinate
R	Dimensionless radial component of coordinate
Ra	Rayleigh number
Re	Reynolds number
T	Dimensionless temperature
u	r component of velocity
U	Dimensionless R component of velocity
v	y component of velocity
V	Dimensionless Y component of velocity
y	Vertical component of coordinate
Y	Dimensionless vertical component of coordinate

Greek symbols

ρ	Density of fluid
β	Thermal expansion coefficient of fluid
ν	Effective kinematic viscosity of fluid
α	Thermal diffusivity
ε	Porosity
θ	Temperature
δ	Height and thickness of annular enclosure
γ	Dimensionless heat generation parameter
λ	Ratio of effective conductivities
μ	Effective dynamic viscosity
ψ	Stream function

Subscripts

f	Fluid phase
s	Solid phase

w	Wall of annular enclosure
o	Outer radios of annular enclosure
i	Inner radios of annular enclosure

References

1. Nield, D.A. and Bejan, A., *Convection in Porous Media*, 3rd Ed., Springer, New York (2006).
2. Ingham, D.B. and Pop, I., Eds., *Transport Phenomena in Porous Media*, Elsevier Science, Oxford (1998).
3. Ingham, D.B. and Pop, I., Eds., *Transport Phenomena in Porous Media III*, Elsevier Science, Oxford (2005).
4. Pop, I. and Ingham, D.B., *Convective Heat Transfer: Mathematical and Computational Modelling of Viscous Fluids and Porous Media*, Pergamon, Oxford (2001).
5. Vafai, K., Ed., *Handbook of Porous Media*, 2nd Ed., Taylor and Francis, New York (2005).
6. Ingham, D.B., Bejan, A., Mamut, E. and Pop, I., Eds., *Emerging Technologies and Techniques in Porous Media*, Kluwer, Dordrecht (2004).
7. Mealey, L.R. and Merkin, J.H. "Steady finite Rayleigh number convective flows in a porous medium with internal heat generation", *International Journal of Thermal Sciences*, **48**, pp. 1068-1080 (2009).
8. Tahmasebi Kohyani, M., Ghasemi, B. and Pasandideh Fard, A. "Heat generation effects on natural convection in porous cavity with different walls temperature", *Frontiers in Heat and Mass Transfer (FHMT)*, **3**, 023008 (2012).
9. Du, Z.G. and Bilge, E. "Natural convection in vertical cavities with partially filled with heat-generating porous media", *Numerical Heat Transfer*, **18**, Part A, pp. 371-386 (1990).
10. Kim, G.B., Hyun, J.M. and Kwak, H.S. "Buoyant convection in a square cavity partially filled with heat-generating porous medium", *Numerical Heat Transfer*, **40**, Part A, pp. 601-618 (2001).
11. Kim, G.B. and Hyun, J.M. "Buoyant convection of a power-law fluid in an enclosure filled with heat-generating porous media", *Numerical Heat Transfer*, **45**, Part A, pp. 569-582 (2004).
12. Rao, Y.F. and Wang, B.X. "Natural convection in vertical porous enclosures with internal heat generation", *Int. J. Heat Mass Transfer*, **34**, pp. 247-252 (1991).
13. Haajizadeh, M., Ozguc, A.F. and Tien, C.L. "Natural convection in a vertical porous enclosure with internal heat generation", *Int. J. Heat Mass Transfer*, **27**, pp. 1893-1902 (1984).
14. Stewart, W.E., Greer, M.E. and Stickler, L.A. "Heat transfer in a partially insulated rectangular enclosure of heat generating porous media", *Int. Comm. Heat Mass Transfer*, **17**, pp. 597-607 (1990).
15. Joshi, M.V., Gaitonde, U.N. and Mitra, S.K. "Analytical study of natural convection in a cavity with volumetric heat generation", *ASME J. Heat Transfer*, **128**, pp. 176-182 (2006).
16. Magyari, E., Pop, I. and Postelnicu, A. "Effect of the source term on steady free convection boundary layer flows over a vertical plate in a porous medium", Part I, *Transport in Porous Media*, **67**, pp. 49-67 (2007).
17. Magyari, E., Pop, I. and Postelnicu, A. "Effect of the source term on steady free convection boundary layer flows over a vertical plate in a porous medium", Part II, *Transport in Porous Media*, **67**, pp. 189-201 (2007).
18. Vafai, K. and Tien, C.L. "Boundary and inertia effects on flow and heat transfer in porous media", *Int. J. Heat Mass Transfer*, **24**, pp. 195-203 (1981).
19. Chen, C.K. and Lin, C.R. "Natural convection from an isothermal vertical surface embedded in a thermally stratified high-porosity medium", *Int. J. Eng. Sci.*, **33**, pp. 131-138 (1995).
20. Alazmi, B. and Vafai, K. "Constant wall heat flux boundary conditions in porous media under local thermal non-equilibrium conditions", *International Journal of Heat and Mass Transfer*, **45**, pp. 3071-3087 (2002).
21. Gunn, D.J. "Transfer of heat or mass to particles in fixed and fluidized beds", *Int. J. Heat and Mass Transfer*, **21**, pp. 467-476 (1978).
22. Joel, H. Ferziger, Milovan Peric, *Computational Methods for Fluid Dynamics*, Springer Publications (2002).
23. Ghia, U., Ghia, K.N. and Shin, C.T. "High-Re solutions for incompressible flow using the Navier-Stokes equations and a Multigrid method", *Journal of Computational Physics*, **48**, pp. 387-411 (1982).
24. Reima Iwatsu, Jae Min Hyun, Kunio Kuwahara, "Mixed convection in a driven cavity with a stable vertical temperature gradient", *Int. J. of Heat Transfer*, **36**, pp. 1601-1608 (1993).
25. Lemembre, A. and Petit, J.-P. "Laminar natural convection in a laterally heated and upper cooled vertical cylindrical enclosure", *Inf J. Hear Mass Transfer*, **41**(16), pp. 2437-2454 (1998).
26. Tanmay Basak, Roy, S., Paul, T. and Pop, I. "Natural convection in a square cavity filled with a porous medium: Effects of various thermal boundary conditions", *International Journal of Heat and Mass Transfer*, **49**, pp. 1430-1441 (2006).
27. Mohammad, A.A. "Non-equilibrium natural convection in a differentially heated cavity filled with a saturated porous matrix", *Journal of Heat Transfer*, **122**, pp. 380-384 (2000).
28. Fumei Rong, Zhaoli Guo, Zhenhua Chai, Baochang Shi, "A lattice Boltzmann model for axisymmetric

thermal flows through porous media", *International Journal of Heat and Mass Transfer*, **53**, pp. 5519-5527 (2010).

29. Batchelor, G.K., *An Introduction to Fluid Dynamics*, Cambridge University Press (1993).

Biographies

Morteza Taherzadeh Fard received his BSc degree in Mechanical Engineering (heat and flow) from University of Kashan in 2007, and his MSc degree in Nuclear Engineering from Sharif University of Technology in 2009, where he is now a PhD student in the same field. His research interests include: safety analysis of nuclear reactors, study of thermal hydraulic parameters of nuclear reactors, two phase flow and multi-phase flow in porous media.

Mohammad Said Saidi received his BSc degree in Physics from Sharif University of Technology in 1973, his MSc degree in Nuclear Engineering from Massachusetts Institute of Technology in 1976, and his PhD degree in Nuclear Engineering from MIT in 1979. He is now professor of mechanical engineering at SUT. His research interests include: fluid mechanics and thermal fluids